

Dealloying/exsolution-induced nanoporous perovskite oxides anchored with alloy nanoparticles for oxygen evolution reaction

Yu Cui^a, Yang Chao^a, Jianbin Lin^a, Wenxue Ke^a, Xin He^a, Mei Chen^a, Chi Zhang^{a,*}

^a School of Applied Physics and Materials, Wuyi University, 99 Yingbin Road, Jiangmen 529020, China

Corresponding author: Chi Zhang: chizhang@wyu.edu.cn, ch.zhang@outlook.com

1. Supplementary figures:

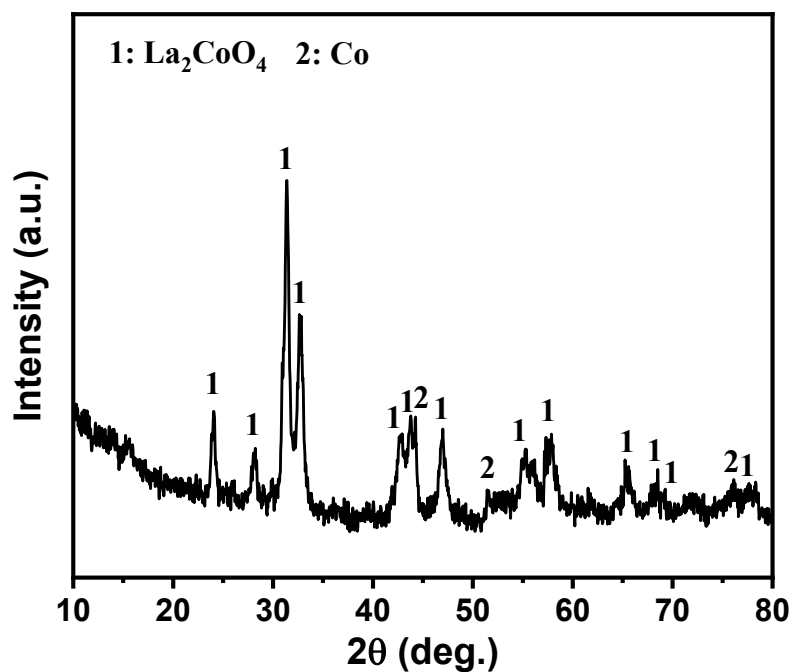


Figure S1. XRD patterns of reduced LaCoO₃ in 5% H₂/Ar at 700 °C for 1 h.

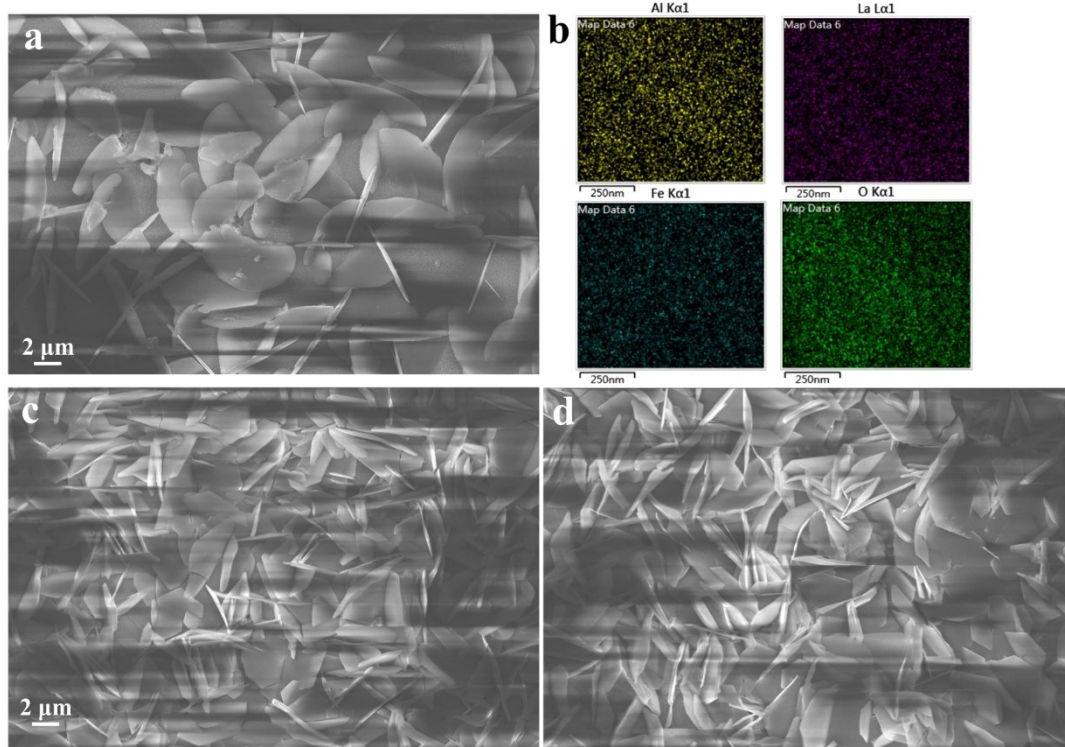


Figure S2: Dealloyed samples of (a) $d\text{-Al}_{88.4}\text{La}_{5.4}\text{Fe}_6$, (b) $d\text{-Al}_{88.4}\text{La}_{5.4}\text{Co}_{0.6}\text{Fe}_{5.4}$, and (c) $d\text{-Al}_{88.4}\text{La}_{5.4}\text{Co}_{1.2}\text{Fe}_{4.8}$.

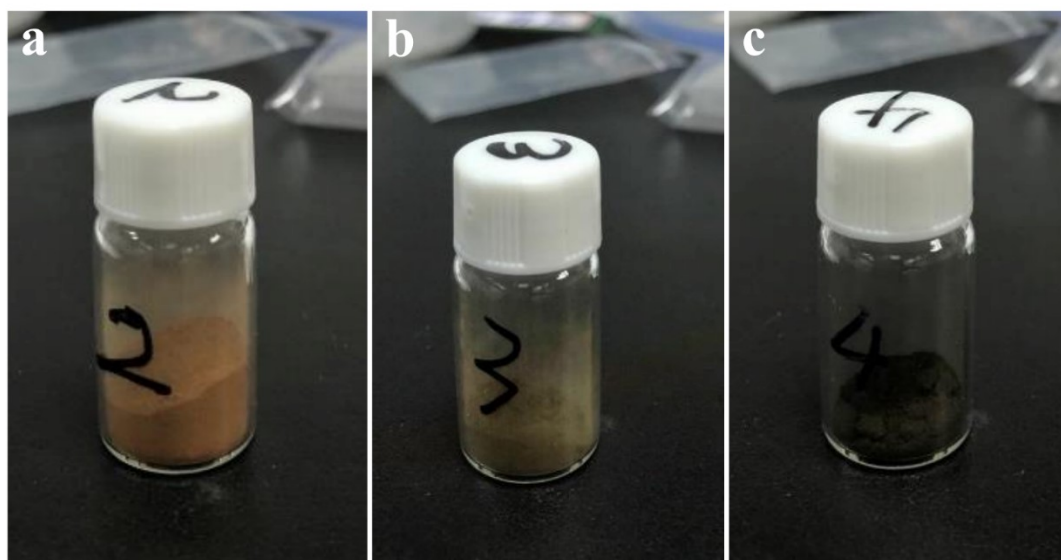


Figure S3. Photo of annealed samples: (a) LF, (b) LCF19, and (c) LCF28.

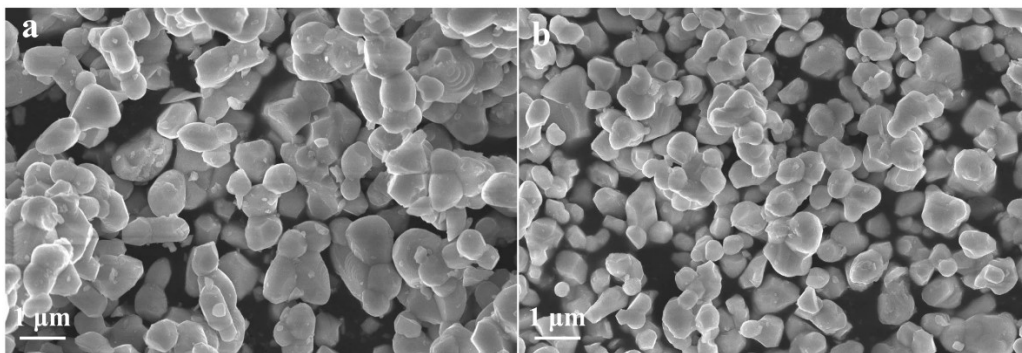


Figure S4. LCF19 synthesized through (a) sol-gel and (b) solid-state reaction method.

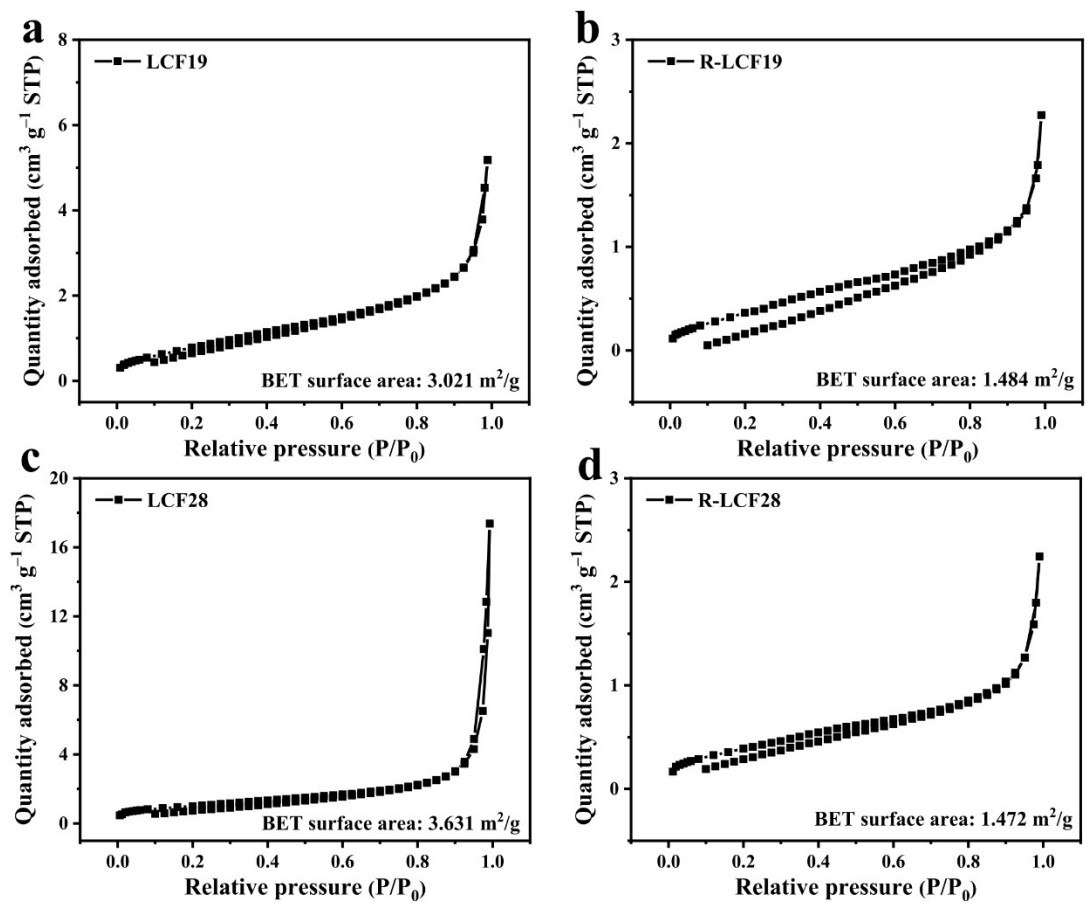


Figure S5. Nitrogen adsorption/desorption isotherms of (a) LCF19, (b) R-LCF19, (c) LCF28, and (d) R-LCF28.

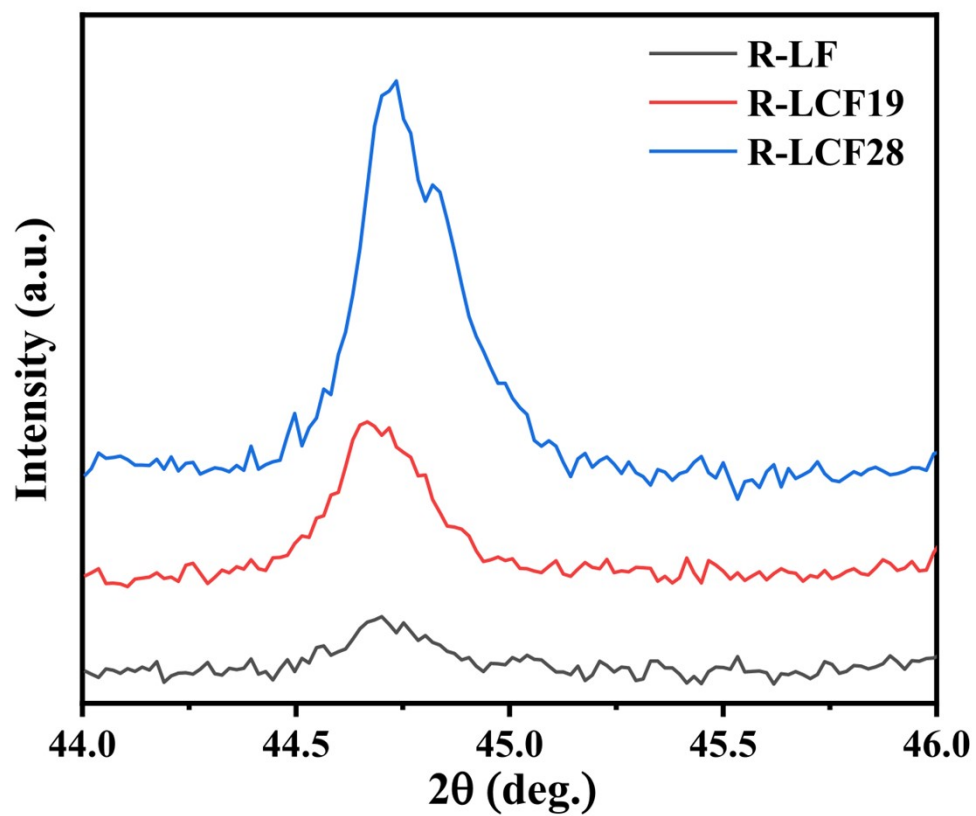


Figure S6. XRD pattern of R-LF, R-LCF19, and R-LCF28 between 44 to 46 degree (2θ).

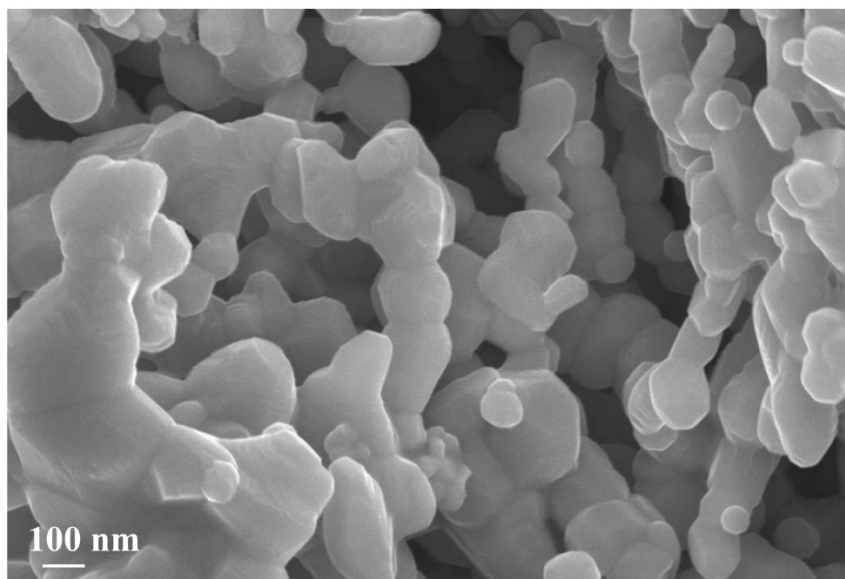


Figure S7. SEM image of LCF19 of high magnification.

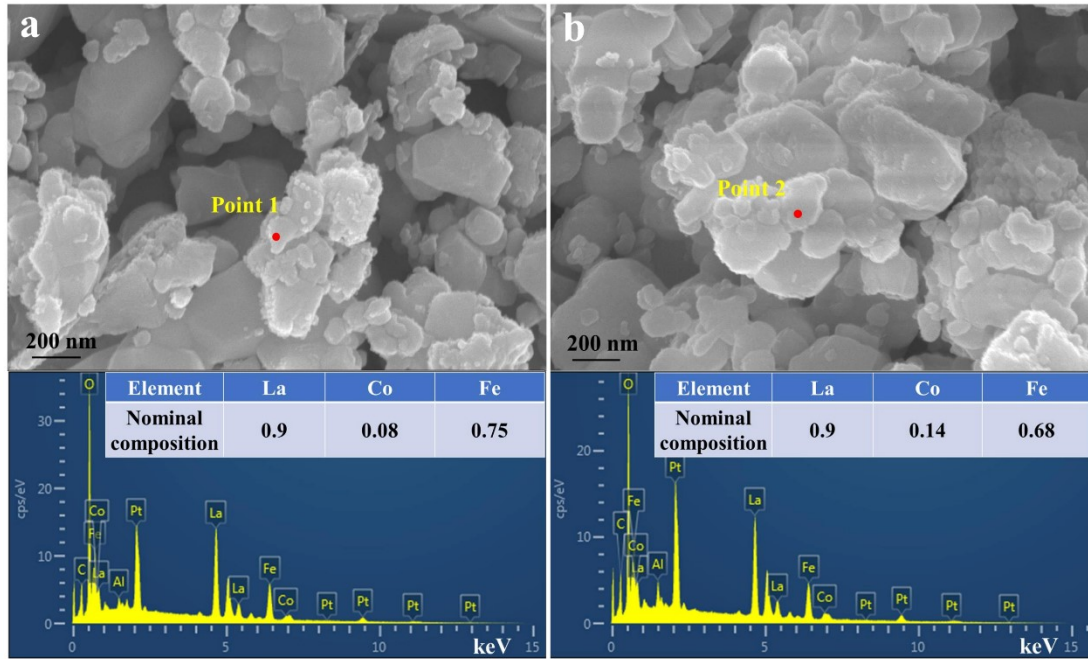


Figure S8. The SEM and EDS spectra of (a) R-LCF19 and (b) R-LCF28.

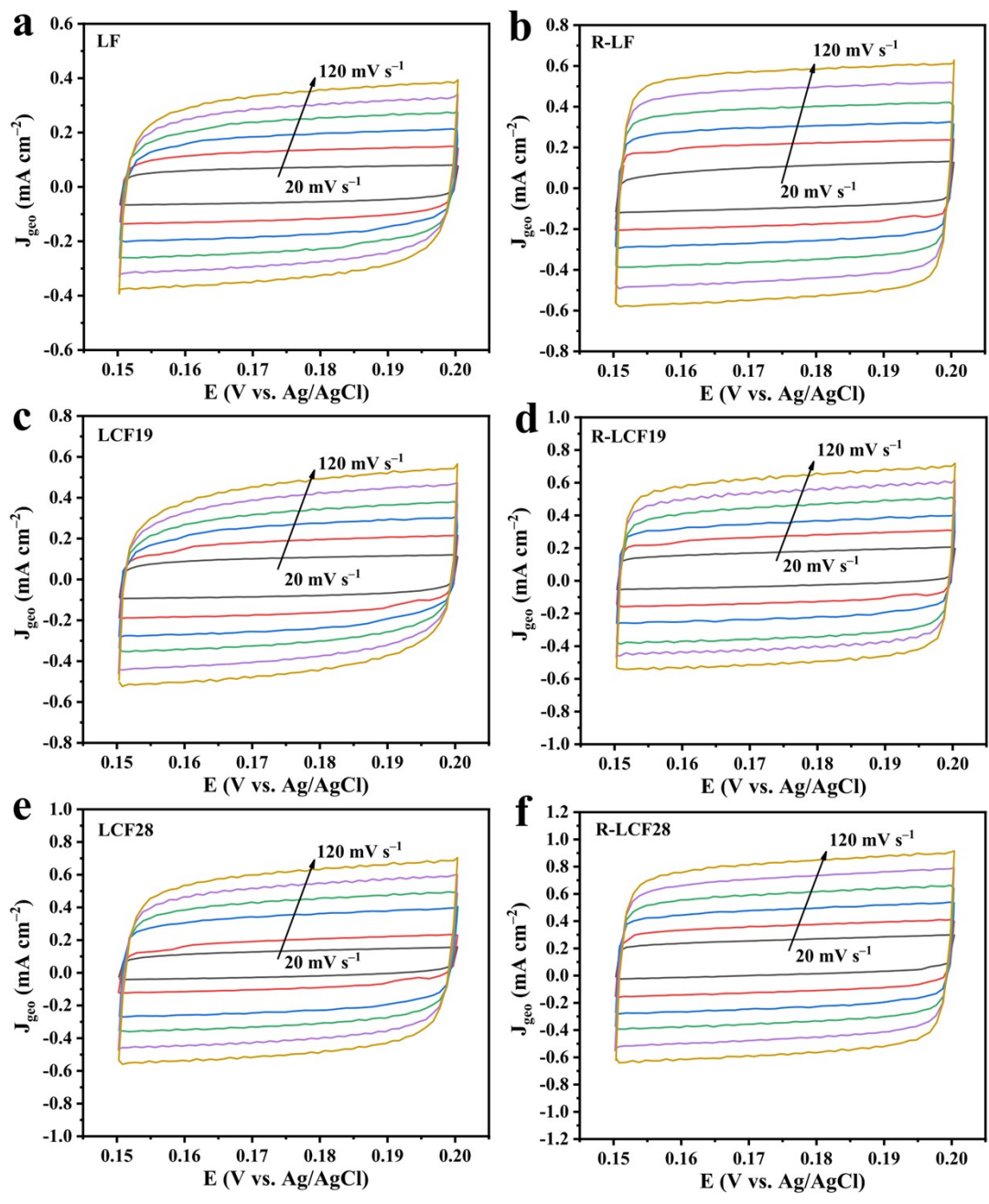


Figure S9. CV curves scanning at different scan rates between 20-120 mV s^{-1} for LF, R-LF, LCF19, R-LCF19, LCF28, and R-LCF8.

2. Supplementary tables:

Table S1 Concentration of La, Co, and Fe calculated by ICP-OES.

Sample	Element content (wt. %)			Element content (at. %)		
	La	Co	Fe	La	Co	Fe
R-LF	67.47	/	32.53	45.47	/	54.53
R-LCF19	68.35	3.50	28.15	46.62	5.63	47.75
R-LCF28	66.95	6.98	26.07	45.15	11.10	43.75

Table S2. The fitted equivalent circuit values of the catalysts.

Catalysts	R_s (Ω)	R_{ct} (Ω)
LF	5.36	73.05
R-LF	5.44	45.32
LCF19	4.93	58.31
R-LCF19	5.43	30.85
LCF28	5.16	57.39
R-LCF28	4.79	11.62